Effective theory of quantum black holes

E. Binetti,[1,*] M. Del Piano,[2,3,†] S. Hohenegger,[4,‡] F. Pezzella,[3,§] and F. Sannino[1,2,3,5,6,‖]

[1]*Department of Physics E. Pancini, Universita di Napoli Federico II, via Cintia, 80126 Napoli, Italy*
[2]*Scuola Superiore Meridionale, Largo S. Marcellino, 10, 80138 Napoli NA, Italy*
[3]*INFN sezione di Napoli, via Cintia, 80126 Napoli, Italy*
[4]*Institut de Physique des 2 Infinis (IP2I), CNRS/IN2P3, UMR5822, 69622 Villeurbanne, France Université de Lyon, Université Claude Bernard Lyon 1, 69001 Lyon, France*
[5]*CP[3]-Origins and D-IAS, Southern Denmark University, Campusvej 55, 5230 Odense M, Denmark*
[6]*CERN, Theoretical Physics Department, 1211 Geneva 23, Switzerland*

(Received 9 June 2022; accepted 28 July 2022; published 23 August 2022)

We explore the quantum nature of black holes by introducing an effective framework that takes into account deviations from the classical results. The approach is based on introducing quantum corrections to the classical Schwarzschild geometry in a way that is consistent with the physical scales of the black hole and its classical symmetries. This is achieved by organizing the quantum corrections in inverse powers of a physical distance. By solving the system in a self-consistent way we show that the derived physical quantities, such as event horizons, temperature and entropy can be expressed in a well-defined expansion in the inverse powers of the black hole mass. The approach captures the general form of the quantum corrections to black hole physics without requiring us to commit to a specific model of quantum gravity.

DOI: 10.1103/PhysRevD.106.046006

I. INTRODUCTION

Understanding the quantum nature of space-time is an open challenge both from a theoretical and an experimental point of view. Quantum gravity effects are thought to be relevant, for example, in gravitational collapse of astrophysical objects as well as evaporation processes of Planck-size black holes (BH). The goal of this work is to construct an effective framework that allows to investigate quantum corrections for BH physics in order to extract reliable predictions. Effective approaches have been applied extensively to account for quantum corrections in gravity and particle physics, see [1] for an overview.

Rather than considering a specific theory of quantum gravity, our philosophy is to develop a general effective framework based on formulating BH metrics via dimensionless quantities and their physical scalings (see [2–4] for related ideas in different areas of physics). Although this approach can be viewed as a renormalization improvement [5–11] of the BH metrics, it differs from the Wilsonian interpretation [12,13] of the running of couplings of the effective action [14] further explored in [15], and therefore it is compatible with the arguments of Ref. [16].

We elucidate our approach by focusing on the static spherically symmetric classical Schwarzschild BH. After introducing the approach, we determine the impact of the leading order quantum corrections on the physical quantities such as event horizons, temperature and entropy in a consistent fashion. In the way the framework is setup, quantum corrections to physical observables appear as a well-defined expansion in the mass of the BH relative to the classical results. We show that the approach can be consistently generalized to higher order quantum corrections leading to higher mass suppressed corrections. Although we do not discuss it in this work, our approach can be further generalized to account for nonlocal corrections to effective gravity actions [17–32]. Our findings amount to establishing a self-consistent effective counting scheme, based on the physical mass of the BH.

The work is organized as follows. In Sec. II we start by introducing the effective framework and by setting up the notation. The section is further divided into several subsections. The rationale behind our way to upgrade the classical metric to an effective quantum one is summarized in the first subsection. We then move to determine the leading order quantum corrected horizons and discuss their impact on the BH physics. We show that, depending on the sign of the first leading order corrections, the geometry can develop a second (internal) horizon. We then move to show the associated conformal diagrams. The self-consistency of the approach, when considering the backreaction stemming from the quantum corrected proper distance, is presented in

*e.binetti@studenti.unina.it
†manuel.delpiano-ssm@unina.it
‡s.hohenegger@ipnl.in2p3.fr
§franco.pezzella@na.infn.it
‖sannino@cp3.sdu.dk

Sec. II D. In Sec. III we discuss how to take into account higher order quantum gravity corrections to the metric. One of the main results is establishing an effective consistent framework in computing quantum corrections to BH physics organized in their mass expansion.

The quantum corrected thermodynamic properties, such as temperature and entropy, are discussed in Sec. IV. Conclusions and outlook are offered in Sec. V while in the Appendix we provide further details on how to compute the horizons in our framework.

II. QUANTUM SCHWARZSCHILD BLACK HOLE

We focus on the simplest BH in four dimensions, featuring a spherical and stationary geometry with Schwarzschild metric

$$\mathrm{d}s^2 = -f_0(r)\mathrm{d}t^2 + \frac{\mathrm{d}r^2}{f_0(r)} + r^2\mathrm{d}\theta^2 + r^2\sin^2\theta\mathrm{d}\phi^2, \quad (1)$$

where we use spherical coordinates and the metric tensor depends only on the radial one through the function

$$f_0(r) = 1 - \frac{2G_N M}{r}, \quad (2)$$

with M being the mass sourcing the gravitational field and G_N the Newton constant.

A. Quantum framework

We now upgrade the metric (1) to a quantum one without committing to a specific underlying quantum gravity theory.[1] At the classical level the metric depends on two dimensionful quantities,[2] the mass of the BH and the coordinate r. In the following we describe the quantum framework that we employ to determine quantum corrections to BH observables.

(1) The quantum corrections are controlled by the Planck length $\ell_P = 1/M_P$ (with M_P the Planck mass), which governs the transition from the classical to the quantum regime. As such, now ℓ_P is upgraded to a physically relevant length beyond providing just a unit of measure. To reflect this, we introduce the following dimensionless quantities:

$$z := M_P r = \frac{r}{\ell_P}, \qquad \chi := \frac{M}{M_P}, \quad (4)$$

and rewrite (2) as:

$$f_0(z) = 1 - \frac{2\chi}{z}g, \quad \text{with} \quad g := G_N M_P^2 = 1. \quad (5)$$

(2) Transitioning from the classical to the quantum regime requires to modify (5) as follows:

$$f\left(z, \frac{u}{\ell_P}\right) = 1 - \frac{2\chi}{z} g\left(z, \frac{u}{\ell_P}\right), \quad (6)$$

where g is an *a priori* undetermined function.[3] Here u is an arbitrary renormalization scale required to compensate for the presence of a fundamental length in the problem, i.e., ℓ_P. Since u is arbitrary no physical quantity can depend on it. This means that the derivative of any such quantity with respect to u must vanish, therefore imposing nontrivial consistency conditions also on $g(z, \frac{u}{\ell_P})$ (see, e.g., [2] for similar arguments in other physical systems). In order for any allowed coordinate transformation of $f_0(z)$ to be carried over at the quantum level one has to conclude that g is a protected quantity and therefore:

$$g\left(z, \frac{u}{\ell_P}\right) \to g\left(d, \frac{u}{\ell_P}\right), \quad (7)$$

for a suitable (dimensionless) physical quantity d which is therefore independent of u.

(3) The choice of the physical dimensionless quantity d is not unique. A candidate choice for it is the normalized proper distance from the center of the BH [14]

$$d(z) := \frac{1}{\ell_P}\int_0^{z\ell_P}\sqrt{|\mathrm{d}s^2|} = \int_0^z \frac{\mathrm{d}z'}{\sqrt{|f(z')|}}. \quad (8)$$

The first integral is understood for fixed values of the angular coordinates (θ, ϕ). Notice that, as remarked above, since $d(z)$ cannot depend on u this implies a constraint for $f(z, \frac{u}{\ell_P})$ which restricts the u dependence of $g(d, \frac{u}{\ell_P})$. We note that quantum improvements of the metric based on unphysical quantities such as the radial coordinate z lead to quantum geometries depending on the specific choice of coordinates. This issue was discussed in detail in [33].

[1] At the quantum level, we require the existence of a spherically symmetric metric with a timelike Killing vector. This ensures that the quantum metric still preserves the form (1)

$$\mathrm{d}s^2 = -h(r)\mathrm{d}t^2 + \frac{\mathrm{d}r^2}{f(r)} + r^2\mathrm{d}\theta^2 + r^2\sin^2\theta\mathrm{d}\phi^2. \quad (3)$$

Here f and h are two functions of r. In this work, since we compute static properties we focus on the quantum corrections contained in $f(r)$.

[2] The Planck scale hidden in the Newton constant at the classical level defines the units, and thereby has no influence on the classical physics.

[3] As already in the classical case (2), we do not explicitly exhibit the dependence on χ.

(4) At large proper distances from the BH the function g approaches asymptotically unity. At the quantum level we have, therefore, for $f(z)$:

$$f(z) = 1 - \frac{2\chi}{z}\sum_{n=0}^{\infty}\frac{\Omega_n}{d(z)^{2n}}. \tag{9}$$

The specific values of the dimensionless coefficients $\Omega_n(\frac{u}{\ell_P})$, with $\Omega_0 = 1$, are dictated by a given theory of quantum gravity. The u dependence of the Ω_n coefficients is constrained by requiring physical quantities to be independent on this arbitrary scale. The expansion in (9) is built to incorporate the fact that at large distances the metric must asymptotically approach the classical one (2). The choice of even inverse powers of $d(z)$ comes from our expectation that this quantum metric emerges from a(n effective) quantum gravity action with only even powers of the derivatives. We have also neglected subleading logarithmic terms. The approach can be readily extended to include a different counting scheme if required by more general theories of quantum gravity. A different definition of the physical distance $d(z)$ leads to modified coefficients Ω_n.

(5) By construction (9) is an involved equation for $f(z)$ which we attack in a self-consistent iterative manner: we shall add one order in n of the series at a time and include the backreaction stemming from the corrected $d(z)$ from the previous order. In practice, this procedure mimics the potential expansion of an effective quantum gravity action in local derivative operators. However, the overall approach does not rely on this interpretation and can therefore be further extended to include nonanalytic terms, which we plan to explore in the future.

In the following subsection we start by considering the leading quantum correction.

B. Leading order quantum metric

To determine the leading order quantum corrected function $f_1(z)$, we introduce the classical proper distance $d_0(z)$ given by

$$d_0(z) = \int_0^z \frac{dz'}{\sqrt{|f_0(z')|}} = \int_0^z \frac{dz'}{\sqrt{|1-\frac{2\chi}{z'}|}}. \tag{10}$$

Performing the integration we have

$$d_0(z) = \begin{cases} \pi\chi - 2\chi\tan^{-1}\sqrt{\frac{2\chi}{z}-1} - \sqrt{z(2\chi - z)}, & 0 < z < 2\chi, \\ \pi\chi + 2\chi\tanh^{-1}\sqrt{1-\frac{2\chi}{z}} + \sqrt{z(z-2\chi)}, & 2\chi < z < \infty. \end{cases} \tag{11}$$

The left panel of Fig. 1 is the graphical representation of the integrand in (10) while the right panel represents (11). The integrand (10) has an integrable singularity at $z_S = 2\chi$ yielding a regular proper distance.

Near the center of the BH the distance function behaves like

$$d_0(z) \simeq \frac{2}{3}\frac{z^{3/2}}{\sqrt{2\chi}} + \mathcal{O}\left(\frac{z^{5/2}}{(2\chi)^{3/2}}\right), \tag{12}$$

while a linear dependence is recovered at distances far from the horizon as shown in Fig. 1. The leading order quantum corrected f function reads

$$f_1(z) = 1 - 2\frac{\chi}{z}\left[1 + \frac{\Omega_1}{d_0^2(z)}\right]. \tag{13}$$

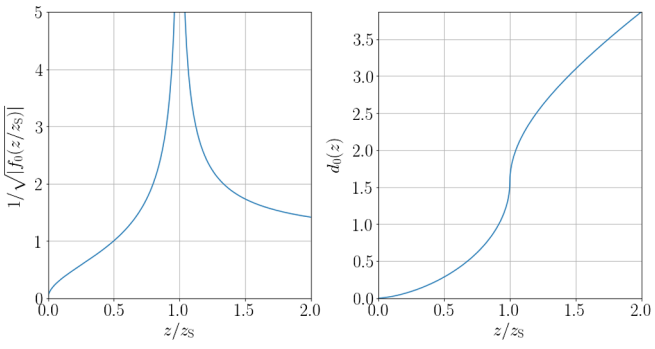

FIG. 1. Left panel: we plot the integrand of (10), normalized to the dimensionless Schwarzschild radius of the BH $z_S = 2\chi$. Right panel: the regular proper distance $d_0(z)$ given in (11).

C. Quantum horizons

We are now ready to discuss the quantum corrections to the BH classical horizon starting with the zeros of $f_1(z)$. Here, the location of the zeroes depends on the sign of the parameter Ω_1 that leads to qualitatively different BH solutions. To remain general, we discuss both cases separately. We plot in Fig. 2 the function $f_1(z)$ for different values of Ω_1 (while we fixed $\chi = 10$). This plot shows two qualitatively very important results

(1) The position of the (external) horizon is a function of Ω_1: positive values of Ω_1 shift the zero of f_1 to larger

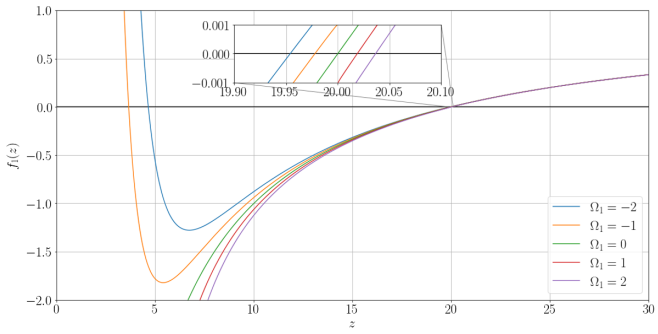

FIG. 2. Plot of the quantum corrected function $f_1(z)$ given in (13) as a function of the distance in Planck units z and for different values of Ω_1 for a fixed mass ratio $\chi = 10$.

values of z, while negative values of Ω_1 move it to smaller values. However, in both cases, the effect is small compared to the classical position of the horizon 2χ, even for values of $|\Omega_1| \geq 1$.

(2) For negative values of Ω_1, the function f_1 allows for a second zero in the physical region $z > 0$, which can be interpreted as the formation of a new *internal horizon*. The position of the latter depends much stronger on the numerical value of Ω_1 than the corrections to the external horizon.

In the following we shall discuss both effects more quantitatively, by treating separately the different signs of Ω_1.

1. $\Omega_1 > 0$

As shown in Fig. 2, for positive values of Ω_1 the function f_1 has a single zero for $z > 0$ corresponding to a single horizon which can be expanded around the classical solution as follows:

$$z_+ = 2\chi\left[1 + \left(\frac{\Omega_1}{\pi^2\chi^2}\right) + \mathcal{O}\left(\frac{\Omega_1}{\pi^2\chi^2}\right)^{3/2}\right] \equiv 2\chi[1 + \alpha + \mathcal{O}(\alpha^{3/2})], \quad \text{with} \quad \alpha := \frac{|\Omega_1|}{\pi^2\chi^2}, \tag{14}$$

We can render α arbitrarily small by increasing χ (the BH mass) for fixed $|\Omega_1|$. While in practice the factor of π^2 in the definition of α in (14) further suppresses the quantum corrections, we remark that $\pi\chi = d_0(2\chi)$ is in fact the classical distance of the classical BH horizon [see Eq. (11)]. Therefore, the expansion in (14) is organized in terms of physical quantities of the classical BH geometry. Naturally, we recover the classical horizon when we either switch off the quantum corrections or increase the BH mass (such that $\alpha \to 0$). We discuss the numerical range of validity of (14) as a function of the BH mass in the Appendix A 1 and higher order corrections in α in the Appendix A 2. As we shall demonstrate in the next subsection, the corrections to z_+ stemming from self-consistently replacing $d_0(z)$ in $f_1(z)$ [see (13)] with

$$d_1(z) = \int_0^z \frac{\mathrm{d}z'}{\sqrt{|f_1(z')|}}, \tag{15}$$

appear at $\mathcal{O}(\alpha^{3/2})$. Therefore, to this order in α, all the quantum corrections are taken into account for the external horizon. The horizon location could depend on the unphysical scale u through Ω_1 which, however, to the current quantum order is constrained to be u independent by requiring d_1 to be a physical quantity to the same order. This can be seen from (A10).

Overall, the horizon increases due to quantum corrections and these are further suppressed at large masses.

2. $\Omega_1 < 0$

In this case the quantum corrected external horizon reads:

$$z_+ = 2\chi[1 - \alpha + \mathcal{O}(\alpha^{3/2})], \tag{16}$$

where α is defined as in (15). The external horizon, now, decreases due to quantum corrections, while the other remarks made for the Ω_1 positive case still apply. For negative values of Ω_1, as shown in Fig. 2, an internal horizon forms at the position

$$z_- = \chi\left(\frac{9\pi}{2}\right)^{1/3}\left[\alpha^{1/3} + \frac{1}{5}\left(\frac{\pi^2}{6}\right)^{1/3}\alpha^{2/3} + \frac{61}{700}\left(\frac{3\pi^4}{4}\right)^{1/3}\alpha + \mathcal{O}(\alpha^{4/3})\right]. \tag{17}$$

Clearly, the existence of the internal horizon has a quantum nature and strongly depends on the underlying theory of quantum gravity.

We display the zeroes of $f_1(z)$ in Fig. 3 as function of χ and observe that the internal horizon is less dependent on this parameter when compared to the external one. Furthermore, for masses close to the Planck value the

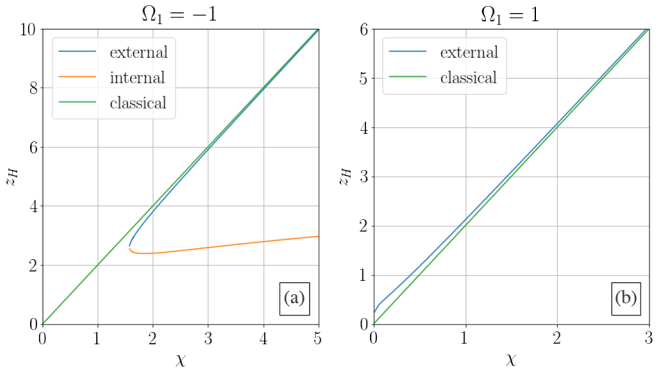

FIG. 3. Black hole event horizons indicated by z_H corresponding to either the classical (straight line), z_+ and z_-, as functions of the mass ratio χ for the value of $\Omega_1 = -1$ (a) and $\Omega_1 = 1$ (b). The values are found solving numerically $f_1(z) = 0$.

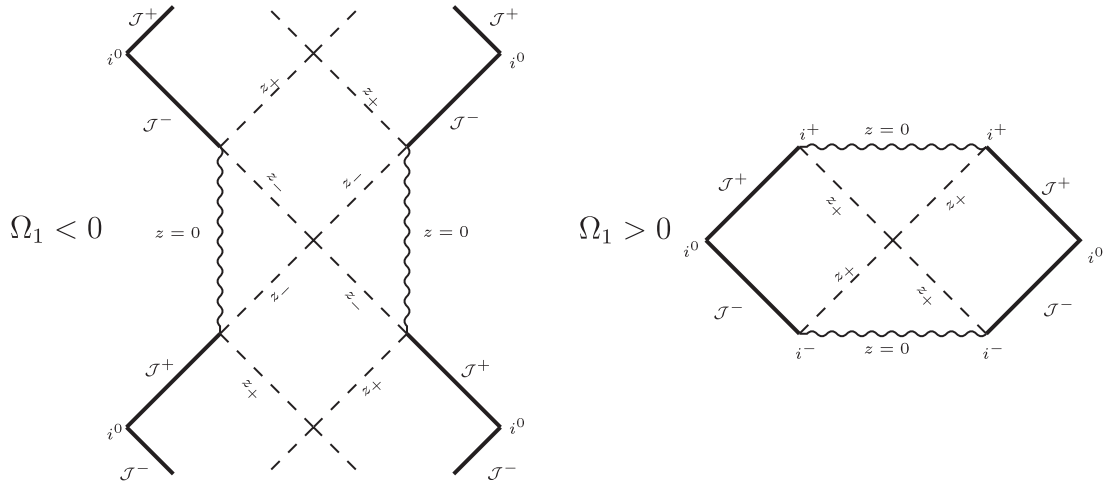

FIG. 4. Conformal diagrams of the quantum corrected space-time described by a metric given by the function in Eq. (13) for $\Omega_1 < 0$ (left) and $\Omega_1 > 0$ (right). The case of negative Ω_1 corresponds to a BH with two distinct event horizons. The notation is the following: $\mathcal{J}^+$ ($\mathcal{J}^-$) is the future (past) null infinity, i^+ (i^-) is the future (past) timelike infinity and i^0 is the spatial infinity, while $z = 0, z_+, z_-$ are respectively the singularity at the origin, the external event horizon and the internal one.

two horizons merge leading to an extremality condition that is analytically approximated to be

$$\chi^{\text{ext}} \simeq \frac{16\sqrt{-\Omega_1}}{\pi^2}. \tag{18}$$

The ultimate fate for the existence of the internal horizon depends, as we shall see, on the size and sign of the higher order corrections.

3. Conformal diagrams

The global properties of the quantum space-time described by the metric with the f function in Eq. (13) can be neatly summarized via Penrose's diagrams [34,35] shown in Fig. 4. The positive Ω_1 case can be summarized as similar to the classical Schwarzschild one with a spacelike singularity while the BH horizon is just slightly larger. The conformal diagram relative to the maximal extension of this space-time is shown in the right panel of Fig. 4, which is the Szekeres-Kruskal conformal diagram [34,35]. Since for negative Ω_1 the quantum BH has two event horizons, its space-time structure qualitatively resembles the classical Reissner-Nordström (RN) one [14,34,35]. To better appreciate the differences we note that, at large distances, the RN dependence on the charge decreases as z^{-2} while for the quantum corrected one it goes as z^{-3} in terms of the quantum effects. The qualitative conformal diagram of the maximal extension of such a space-time is therefore still expected to be of the form given in the left panel of Fig. 4.

As it is shown, the singularity at the origin is a timelike one and the two horizons z_+ and z_- can be crossed by a timelike infalling observer who can reach multiple space-times. The case of an extremal BH is not shown and it can be found in the literature as its conformal diagram, as stated before, is analogous to the classical RN one.

D. Quantum proper distance

Even including only the leading quantum corrections by restricting to an effective second-derivative action (and thus truncating the series (9) at $n = 1$), Eq. (13) is only an approximation, since it contains the classical proper distance d_0. Self-consistency requires to include the impact of the quantum corrected geodesic distance, previously also indicated as proper distance, on the quantum f function given in (13) by substituting d_0 with

$$d_1(z) = \int_0^z \frac{\mathrm{d}z'}{\sqrt{\left|1 - \frac{2\chi}{z'}\left[1 + \frac{\Omega_1}{d_0^2(z')}\right]\right|}}. \tag{19}$$

We therefore obtain the quantum self-improved f function[4]

$$\bar{f}_1(z) = 1 - 2\frac{\chi}{z}\left[1 + \frac{\Omega_1}{d_1^2(z)}\right]. \tag{20}$$

For $\Omega_1 < 0$, one observes that d_1 remains smaller than the classical d_0 for values of z smaller than the internal horizon while it is larger for any other value of z. Nevertheless the qualitative behavior of the quantum distance mimics the classical geodesic one. A similar analysis for $\Omega_1 > 0$ is simplified by the fact that only the external horizon is present. Here the quantum corrected proper distance d_1 again follows the behavior of the

[4]The procedure is straightforwardly generalized when considering higher order quantum corrections, as we shall see below.

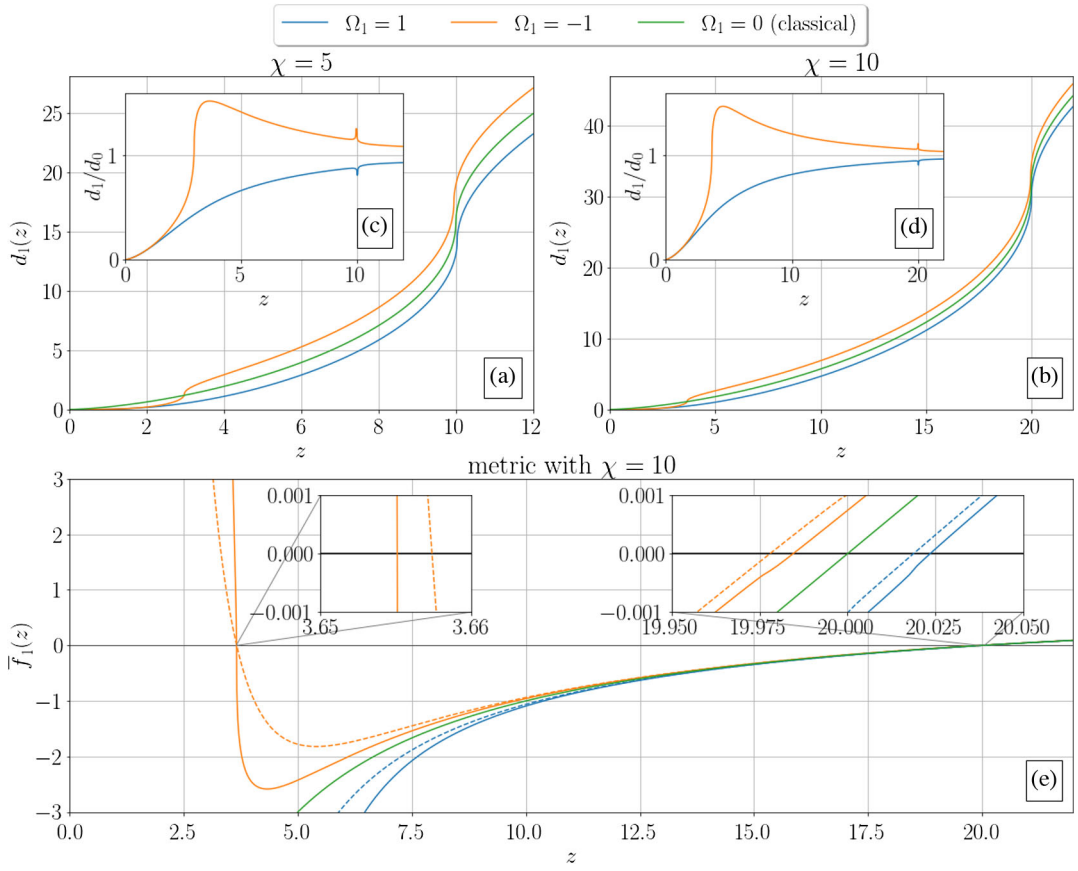

FIG. 5. In the panels (a) and (b) we plot the dimensionless quantum corrected proper distance d_1 for $\Omega_1 = 1$ and $\Omega_1 = -1$, and for two different values of the mass ratio $\chi = 5$ (a), 10 (b). We also plot d_0 corresponding to the classical proper distance ($\Omega_1 = 0$). The ratio d_1/d_0 is displayed in the inserts (c) and (d). In the bottom panel (e) the solid lines (blue for $\Omega_1 > 0$ and orange for $\Omega_1 < 0$) correspond to the improved quantum function $\bar{f}_1(z)$ while the dotted lines correspond to the unimproved $f_1(z)$. The green solid line represents the classical function $f_0(z)$.

classical distance. In panels (a) and (b) of Fig. 5 we display the classical and quantum proper distances. The two plots correspond to two different values of the BH mass. We also observe that near the origin the quantum corrected geodesic distance approaches zero faster than the classical one, specifically it goes as z^3 rather than $z^{3/2}$. For completeness we plot the ratio of d_1/d_0 as function of z in the panels (c) and (d) of Fig. 5 corresponding again to two different choices of the BH mass.

To acquire a general understanding of the effects of the improved results for the function $\bar{f}_1$ of (20) we plot it in Fig. 5. The solid green line corresponds to the classical function f_0, the orange and blue to the different signs of Ω_1 taking into account the quantum corrected proper distance. The dashed curves correspond to the unimproved quantum f function obtained via the classical proper distance. As we had anticipated earlier, the location of the horizons, as shown in Fig. 6, are marginally affected by the improvement due to the quantum proper distance backreaction. Specifically, the quantum proper distance improvement appear, for the external horizon to the $\mathcal{O}(\alpha^{3/2})$, and for the internal one (for Ω_1 negative) a numerical investigation suggests that the improvement appears beyond the order $\mathcal{O}(\alpha)$.

III. HIGHER ORDER QUANTUM CORRECTIONS

After having treated the leading quantum corrections in the previous section, we shall now discuss the procedure to self-consistently consider higher order quantum corrections. That is, we consider higher corrections to the f function, but still truncate the sum in Eq. (9) at a finite n.[5] In this way, we assume that the underlying quantum corrected gravitational theory can be approximated via a local effective action featuring higher derivative operators up to order $2n$. Thus, we expect the resulting f function to assume the form

[5]Notice that by keeping n finite allows us to avoid questions about the radius of convergence of the sum in Eq. (9). The latter is equivalent to the question whether the underlying theory of quantum gravity allows for a nonperturbative definition beyond a (perturbative) effective approach.

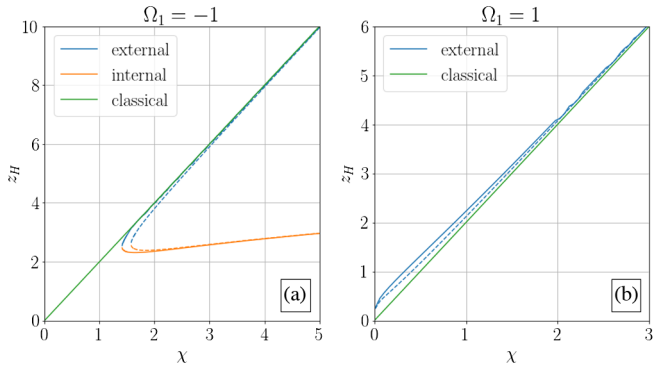

FIG. 6. In the subplot (a) we set $\Omega_1 = -1$ and we represent the external and internal event horizon dimensionless radii z_H as a function of the mass ratio χ in the case of a space-time with backreaction on f described by the function in Eq. (20) (solid lines) and compare them with the ones that come from Eq. (13) (dashed lines). In subplot (b) we study the case in which $\Omega_1 = 1$ and plot the event horizon radius as χ varies and compare it with the one without backreaction on the f discussion. Eventual oscillations in the plots are due to numerical errors.

$$\bar{f}_n(z) = 1 - \frac{2\chi}{z}\left(1 + \frac{\Omega_1}{\bar{d}_n^2(z)} + \frac{\Omega_2}{\bar{d}_n^4(z)} + \cdots + \frac{\Omega_n}{\bar{d}_n^{2n}(z)}\right), \tag{21}$$

with

$$\bar{d}_n(z) = \int_0^z \frac{\mathrm{d}z'}{\sqrt{|\bar{f}_n(z')|}}. \tag{22}$$

To be able to compute this quantity in an iterative manner we approximate it via

$$d_n(z) = \int_0^z \frac{\mathrm{d}z'}{\sqrt{|f_n(z')|}} \equiv \int_0^z \frac{\mathrm{d}z'}{\sqrt{|1 - \frac{2\chi}{z'}(1 + \frac{\Omega_1}{d_{n-1}^2(z')} + \frac{\Omega_2}{d_{n-1}^4(z')} + \cdots + \frac{\Omega_n}{d_{n-1}^{2n}(z')})|}}, \tag{23}$$

where d_{n-1} is the quantum corrected proper distance at order $n-1$.

Even for $n > 1$, there are two limits where the full behavior of d_n as function of z can be studied:

(1) asymptotically large distance: Far away from the black hole d_n approaches z. This limiting behavior is crucial for the self-consistency of our approach: indeed, it is required to match the effective coefficients Ω_n to specific predictions from a given underlying quantum gravity theory. The universality of this limit

$$\lim_{z\to\infty} d_n(z) = \lim_{z\to\infty} d_0(z), \quad \forall\, n \geq 0, \tag{24}$$

ensures that the coefficients $\Omega_{i\leq n}$ can be defined in a consistent fashion, independent of the order n.

(2) distances close to the center of the BH: Here the dominant term in the integrand of (23) is the last term in the denominator. This allows us to deduce, up to a multiplicative number, the following relation

$$\lim_{z\to 0}\frac{d_n}{d_0} \sim \lim_{z\to 0}\frac{d_{n-1}^n}{\sqrt{|\Omega_n|}}, \tag{25}$$

with d_0 computed near the origin of the BH and therefore given by the first term in (12). Iteratively, this relation suggests

$$\lim_{z\to 0} d_n \sim \lim_{z\to 0}\frac{(d_0)^{e\Gamma(n+1,1)}}{\sqrt{\prod_{i=1}^n |\Omega_i|^{n!/i!}}}, \tag{26}$$

where $\Gamma\ (n+1,\ 1)$ is the incomplete Gamma function (and we have implicitly assumed that all $\Omega_{i=1,\ldots,n} \neq 0$). This implies that near the origin, at each given order in n, the truncated physical quantum distance approaches zero extremely fast.

Now, we consider the explicit case of $n = 2$ to learn how it affects our previous results[6]

$$f_2(z) = 1 - \frac{2\chi}{z}\left(1 + \frac{\Omega_1}{d_1^2(z)} + \frac{\Omega_2}{d_1^4(z)}\right). \tag{27}$$

Using (25) we have that

$$\lim_{z\to 0} d_1 \sim \lim_{z\to 0}\frac{d_0^2}{\sqrt{|\Omega_1|}}, \quad \text{and} \quad \lim_{z\to 0} d_2 \sim \lim_{z\to 0}\frac{d_0^5}{|\Omega_2|^{\frac{1}{2}}|\Omega_1|}. \tag{28}$$

Therefore, near the origin the corrections stemming from d_2 do not affect f_2 since they enter at higher orders.[7] In Fig. 7 we compare the quantum function f_2 with the improved $\bar{f}_1$, for different values of $\Omega_1 = \pm 1$ and $\Omega_2 = -0.5,\ 0.2,\ 0.5$. Of course, when comparing with $\bar{f}_1$ we use the same values of Ω_1 appearing in f_2.

We observe that, for both signs of Ω_1, the external horizon expansion works extremely well yielding only minor corrections stemming from f_2 when keeping Ω_2 of order unity. This result is confirmed by the analytic expression of the external horizon in the expansion in the inverse BH mass which reads, for either positive or negative values of $\Omega_{1,2}$:

[6]More details on the analysis can be found in the Appendix A 3.

[7]These limits are also recovered in a slightly different fashion in the Appendix A 3.

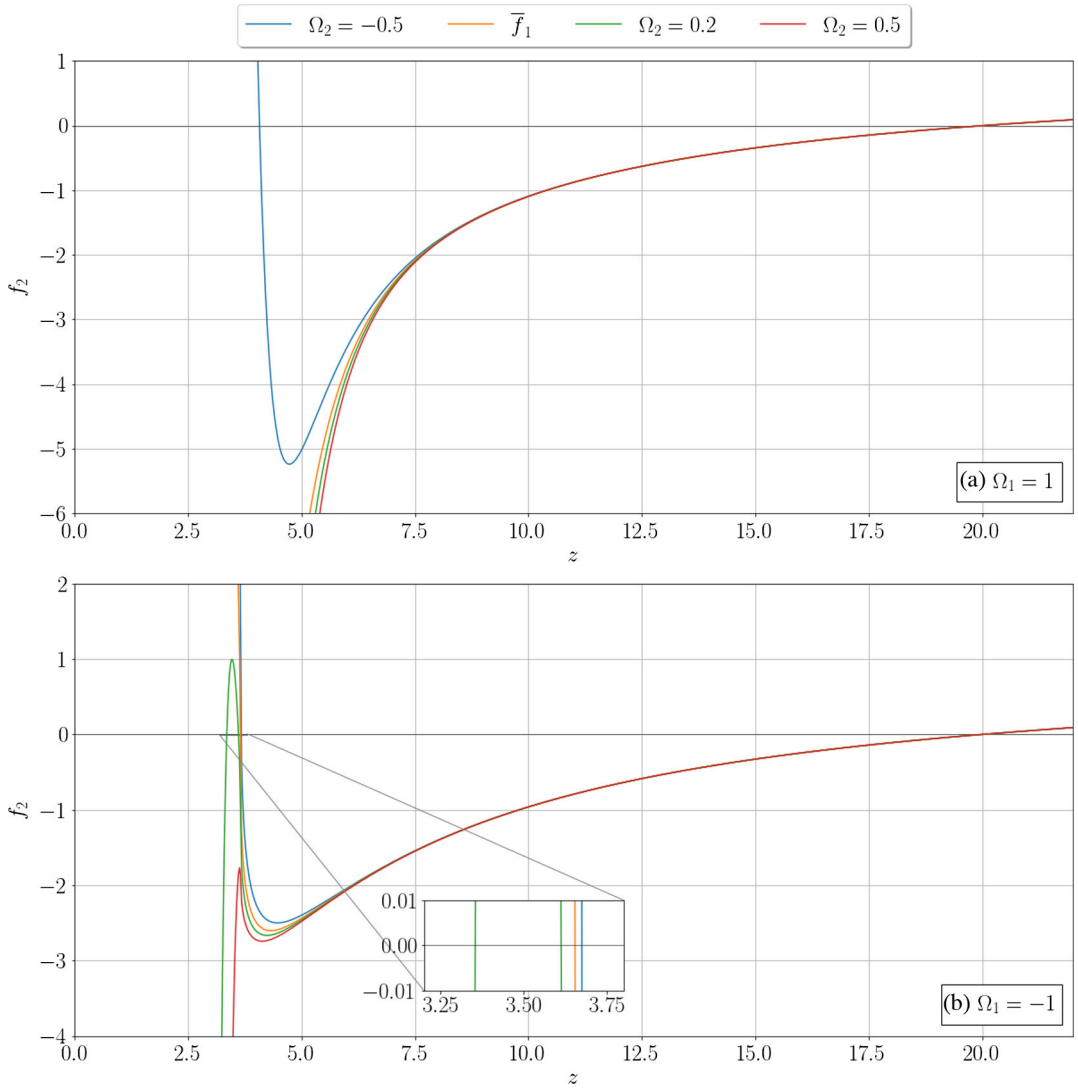

FIG. 7. In top panel (a) we present f_2 for $\Omega_1 = 1$ and three values of Ω_2 as shown in the legend on the top, with the improved function $\bar{f}_1$ displayed as a solid orange line. In the bottom panel (b) is as in (a) but with $\Omega_1 = -1$. In both plots we have set the BH mass relative to the Planck one to $\chi = 10$.

$$z_+ = 2\chi\left[1 + \frac{\Omega_1}{\pi^2\chi^2} + \bar{a}_3\left(\frac{|\Omega_1|}{\pi^2\chi^2}\right)^{3/2} + \bar{a}_4\left(\frac{\Omega_1}{\pi^2\chi^2}\right)^2 + \frac{\Omega_2}{\pi^4\chi^4} + \mathcal{O}\left(\frac{|\Omega_1|^{5/2}, |\Omega_1|^{1/2}\Omega_2}{\pi^5\chi^5}\right)\right]. \tag{29}$$

The leading f_2 corrections appear at the order $\Omega_2/(\pi\chi)^4$ while the corrections stemming from the quantum corrected geodesic d_1 appear at the order $(\Omega_1/(\pi^2\chi^2))^{3/2}$ which is one order less in $1/\pi\chi$, consistently with this expansion. The coefficient $\bar{a}_3/4$ of $(\Omega_1/(\pi^2\chi^2))^{3/2}$ is numerically evaluated in the Appendix A 2 (see Eq. (A3) for $\Omega_1 > 0$ and Eq. (A4) for $\Omega_1 < 0$).

The situation changes for the interior of the BH: as shown in Fig. 7, the structure of zeroes of the function f_2 depends crucially on the sign and magnitude of Ω_2 (and Ω_1). The BH geometry can therefore have zero, one or two internal horizons. Concretely, the phase diagram, representing the regions in the (Ω_1, Ω_2) plane featuring different numbers of internal horizons stemming from the f_2 function, is shown in Fig. 8 for $\chi = 5$ in the left panel (a) and $\chi = 10$ in the right panel (b). One observes that the majority of the phase diagram features either none (upper pink region) or at most one (lower orange region) internal horizon. The light blue region supports two internal horizons.

IV. THERMODYNAMICS

So far we investigated the static properties of the BH in the effective quantum regime. We now move to determine its leading quantum thermodynamic properties.

We start by computing the Hawking's [36] equilibrium temperature around the external horizon via its surface

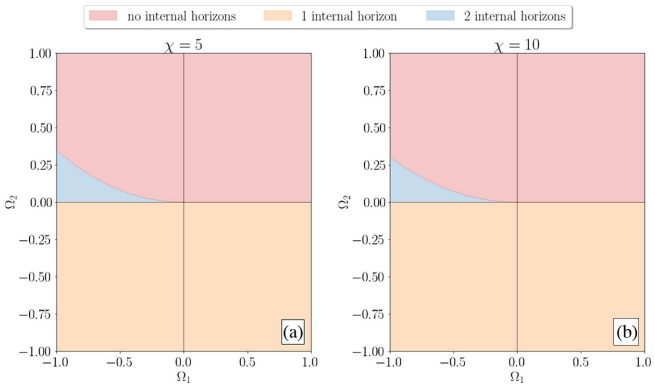

FIG. 8. Phase diagram defining the regions in the (Ω_1, Ω_2) plane with different numbers of internal horizons emerging from the quantum function f_2 for $\chi = 5$ (panel a) and $\chi = 10$ (panel b).

gravity parameter κ. For the present BH metric the temperature is given in terms of the f function, by

$$T_{\rm H} = \frac{\kappa}{2\pi} = \frac{1}{4\pi}\frac{{\rm d}f(r)}{{\rm d}r}\bigg|_{r=r_+}, \tag{30}$$

where r_+ is the radius of the external event horizon. Specializing this expression to the case in (13) with $r_+ = \ell_{\rm P} z_+$, we have

$$T_{\rm H} = \frac{1}{4\pi\ell_{\rm P}}\left[\frac{2\chi}{z_+^2}\left(1 + \frac{\Omega_1}{d_0(z_+)^2}\right) + \frac{4\chi}{z_+}\frac{\Omega_1}{d_0(z_+)^3}\frac{{\rm d}d_0}{{\rm d}z}\bigg|_{z=z_+}\right]. \tag{31}$$

The prefactor

$$T_{\rm P}^{(0)} = \frac{1}{4\pi\ell_{\rm P}}, \tag{32}$$

can be naturally interpreted as the Hawking temperature for a classical Schwarzschild BH of Planck mass. From now on, we shall therefore work with the normalized ratio $T_{\rm H}/T_{\rm P}^{(0)}$.

As expected, for large enough values of χ, the temperature in Eq. (31) tends to the *semiclassical* one, which is defined as

$$\frac{T_{\rm H}^{(0)}}{T_{\rm P}^{(0)}} = \frac{1}{2\chi}. \tag{33}$$

This is shown in Fig. 9. The consistent quantum expansion of Eq. (31) reads:

$$\frac{T_{\rm H}}{T_{\rm P}^{(0)}} = \begin{cases} \frac{1}{2\chi}\left[1 - \frac{4}{\pi^2}\frac{\sqrt{|\Omega_1|}}{\chi} + \left(1 - \frac{48}{\pi^2}\right)\frac{|\Omega_1|}{\pi^2\chi^2} + \mathcal{O}\left(\left(\frac{|\Omega_1|}{\pi^2\chi^2}\right)^{3/2}\right)\right] & \Omega_1 < 0, \\ \frac{1}{2\chi}\left[1 + \frac{4}{\pi^2}\frac{\sqrt{|\Omega_1|}}{\chi} - \left(1 + \frac{48}{\pi^2}\right)\frac{|\Omega_1|}{\pi^2\chi^2} + \mathcal{O}\left(\left(\frac{|\Omega_1|}{\pi^2\chi^2}\right)^{3/2}\right)\right] & \Omega_1 > 0. \end{cases} \tag{34}$$

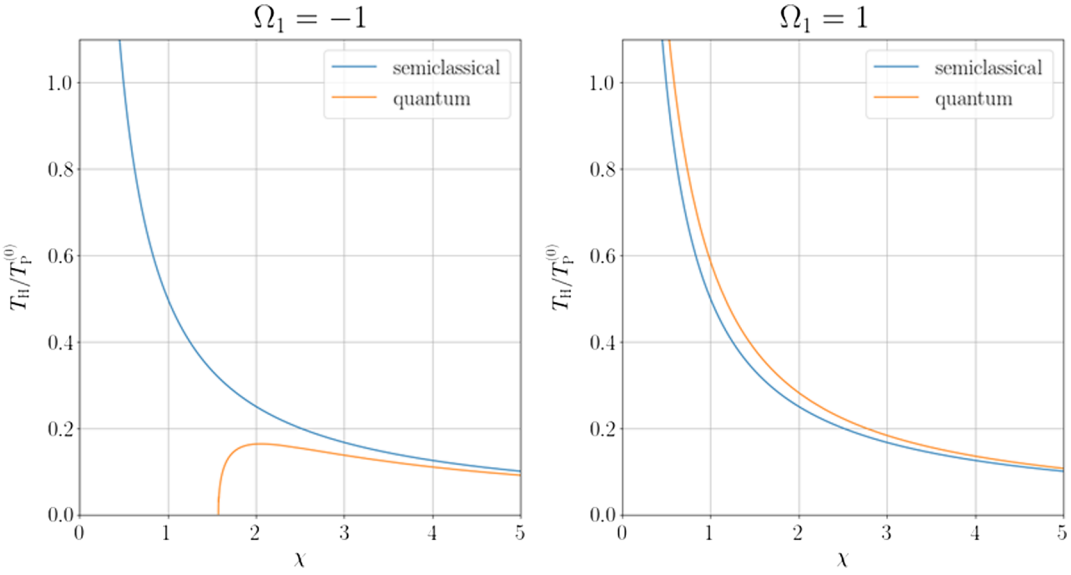

FIG. 9. We plot the value of the Hawking temperature ratio $T_{\rm H}/T_{\rm P}^{(0)}$ as a function of χ in the case for $\Omega_1 = -1$ (left) and $\Omega_1 = 1$ (right). It is noticeable that the temperature drops to zero at the extremal value of the mass while the *(semi)*classical result continues evaporating.

At the quantum level the corrected BH temperature decreases or increases, depending on whether the first order corrections to the metric are negative or positive. Additionally, in contrast to the classical case the decrease (increase) to the external horizon due to the quantum corrections leads to a decrease (increase) in the associated quantum temperature.

Although our counting scheme for quantum corrections limits the validity of our analysis to the results above it is interesting to discuss the small χ limit for negative Ω_1. We consider still the leading order correction to the metric [i.e., we consider $n = 1$ in Eq. (9)], which we approximate as (12). In this case, the quantum BH temperature achieves a maximum around $\chi \sim 2$ and rapidly decreases to zero for smaller χ. At this point the internal and external horizons merge and the BH becomes extremal (18). If this picture holds for the full quantum result this would suggest that the evaporation process leaves behind a stable remnant rather than observing a complete evaporation of the BH. We hasten to add, however, that higher order corrections cannot consistently be neglected in this regime and may qualitatively change the picture.

We finally turn our attention to the BH entropy S which is obtained by integrating the first law of BH thermodynamics

$$\mathrm{d}M = T_{\mathrm{H}}\mathrm{d}S \Rightarrow \mathrm{d}S = \frac{\mathrm{d}M}{T_{\mathrm{H}}} = M_{\mathrm{P}}\frac{\mathrm{d}\chi}{T_{\mathrm{H}}}. \tag{35}$$

The temperature depends on the mass ratio χ once Ω_1 is fixed and therefore we have

$$S = M_{\mathrm{P}}\int \frac{\mathrm{d}\chi}{T_{\mathrm{H}}(\chi)}. \tag{36}$$

Inserting the mass expansion of the temperature in Eq. (34), we have that the entropy assumes, up to a reference value, the following form

$$S = \begin{cases} 4\pi\chi^2\left[1 + \frac{8}{\pi^2}\frac{\sqrt{|\Omega_1|}}{\chi} - 4\left(1 - \frac{64}{\pi^2}\right)\frac{|\Omega_1|}{\pi^2\chi^2}\log\chi + \mathcal{O}\left(\left(\frac{|\Omega_1|}{\pi^2\chi^2}\right)^{3/2}\right)\right] & \Omega_1 < 0, \\ 4\pi\chi^2\left[1 - \frac{8}{\pi^2}\frac{\sqrt{|\Omega_1|}}{\chi} + 4\left(1 + \frac{64}{\pi^2}\right)\frac{|\Omega_1|}{\pi^2\chi^2}\log\chi + \mathcal{O}\left(\left(\frac{|\Omega_1|}{\pi^2\chi^2}\right)^{3/2}\right)\right] & \Omega_1 > 0. \end{cases} \tag{37}$$

Thus, the entropy increases (decreases) for negative (positive) values of Ω_1. The leading quantum correction is linear in χ while only the subleading quantum correction receives corrections in the logarithm of the mass. In fact, the latter vanish at the Planck mass. Logarithmic corrections to the entropy of quantum BHs have also been found by using various other methods, see for example [37–39].

V. CONCLUSIONS

We investigated the quantum nature of black holes by employing an effective approach able to describe quantum deviations from the classical results. We have studied in detail the Schwarzschild black hole, which is the simplest example in four dimensions, however, our approach can readily be extended to other types of geometries (which we plan to discuss in the future). Here we notably assumed that no other physical quantum gravity scale emerges besides the Planck one.

Upon setting up the framework we determined the quantum corrections to the event horizon structure. To leading order in the quantum corrections, and depending on their sign, we showed that the black hole can either have a single horizon or develop a second internal one. We tested the robustness of our results by further considering both the backreaction on the quantum proper distance as well as the effects of higher order corrections. In this way we have demonstrated that the quantum corrections can be consistently organized into expansions dictated by inverse powers of the mass. We also note that these results do not hinge on a particular model of quantum gravity: indeed, different models simply provide specific values of the coefficients Ω_n for the quantum corrections. For example, according to the radiative computations in [40], one would have $\Omega_1 = -167/(30\pi) \sim -1.77$ and therefore the physics is the one stemming from a negative value of Ω_1. Similarly one could match the coefficients to the prediction for the quantum metric stemming from different quantum gravity actions featuring, for example, higher curvature terms such as $f(R)$ theories [41–43]. For a recent discussion about potential constraints on some of the Ω_n coefficients see [44]. Alternatively, in the future, some of these coefficients could be experimentally determined. To further test the robustness of our quantum framework we have shown how to take into account higher order corrections to the metric. We have even provided the explicit form of the next to next leading order quantum corrections to the external horizon. The results demonstrate the effectiveness and reliability of the expansion. We have also observed that the fate of the internal horizon, for Ω_1 negative, is sensitive to higher order corrections. We have consequently provided, to the next-to-next leading quantum order, the parameter space diagram illustrating the various scenarios for the internal horizon. Because of the nature of the expansion in (9) one can only address the ultimate fate of the singularity at the origin of the black hole within a specific model of quantum

gravity which would allow to resum the entire series nonperturbatively. We also provided the conformal diagrams for the quantum corrected black holes and determined the impact of the quantum corrections on the thermodynamic properties such as temperature and entropy.

Our approach differs from the renormalization group improvement of a black hole space time in which the Newton constant is upgraded to an effective running coupling [14,15]. Within this latter framework it has been recently shown [33] that the renormalization group improvement at the level of the metric is coordinate-dependent while the approach is applicable at the level of curvature invariants. Although in our framework we still work at the level of the black hole metric our quantum modified metric depending only on physical quantities leads to coordinate independent observables.

If the quantum scale for gravity turns out to be lower than the Planck scale, our framework can take this into account by a simple rescaling of the dimensionless proper distance used in the definition of the quantum f function of (6). A smaller quantum gravity scale can lead to sizable phenomenological effects.

Overall, we have showed that quantum corrections to black hole physics can be organized in a powerful expansion in their mass that, already at the leading order, allows us to explore the quantum nature of black holes at distances that can be as close to the origin of the black hole, as few times the Planck length. The framework can be employed to investigate quantum corrections for other extended gravitational objects.

ACKNOWLEDGMENTS

We thank Matthias Blau, Alfio Bonanno, Cliff Burgess, Salvatore Capozziello, John Donoghue, Domenico Orlando, Roberto Percacci, Alessia Platania, and Manuel Reichert for comments and/or enlightening discussions.

APPENDIX A: QUANTUM CORRECTED HORIZONS OF THE SCHWARZSCHILD METRIC

1. Range of validity of the quantum corrected horizon position

We provide a numerical estimate of the range of validity of the approximation (14) for the position of the (external) horizon calculated as the zeroes of the f function (12). For simplicity (and since these computations only act as an order of magnitude estimate), we limit ourselves to the case Ω_1. Specifically, we consider the zero (14) as an entire series of the form

$$z_+ = 2\chi \sum_{n=0}^{\infty} a_n \alpha^{n/2}, \quad \text{with} \quad \begin{aligned} a_0 &= 1, \\ a_1 &= 0, \\ a_2 &= 1. \end{aligned} \tag{A1}$$

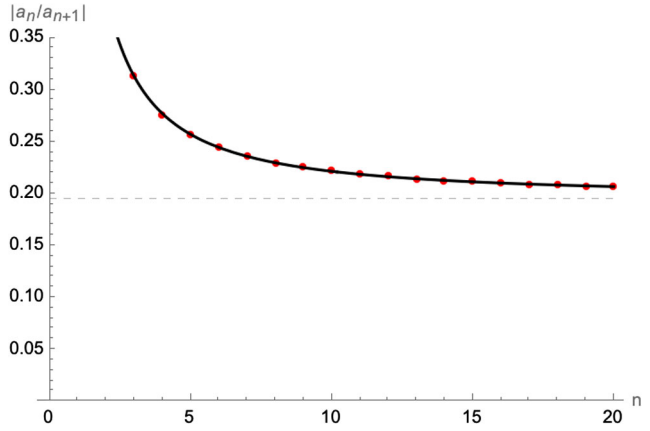

FIG. 10. Absolute value of the quotient $|a_n/a_{n+1}|$ of the coefficients in Eq. (A1). The black line interpolates the coefficients by a function of the form $\frac{a}{n^b} + c$ for $a = 0.475 \pm 0.003$, $b = 1.279 \pm 0.008$ and $c = 0.1968 \pm 0.0004$.

An estimate for the range of validity of the result (14) can be obtained by the radius of convergence of this series. Indeed, in Fig. 10 we have plotted (norm) of the ratio $|a_n/a_{n+1}|$ which asymptotically approaches to the radius of convergence $r \sim 0.1968 \pm 0.0004$. This suggests, that the result (14) can be trusted for BH masses

$$\chi \geq \frac{\sqrt{\Omega_1}}{\pi\sqrt{r}} \sim 0.718\sqrt{\Omega_1}. \tag{A2}$$

2. Numerical calculation of the position of the horizon(s)

Here we perform a numerical analysis of the zeroes of the quantum self-improved metric function (20) with d_1 defined in (19). We are in particular interested in the order in the parameter α [defined in Eq. (14)] at which this modification changes the position of the horizon(s) of the black hole compared to f_1 defined in (13). To this end, we distinguish the cases $\Omega_1 > 0$ and $\Omega_1 < 0$

(i) $\Omega_1 > 0$: In this case, the zeroes of $\bar{f}_1$ as a function of α (for $\chi = 2$) are plotted in Fig. 11 for the choice $\chi = 2$. The solid black line is approximated by

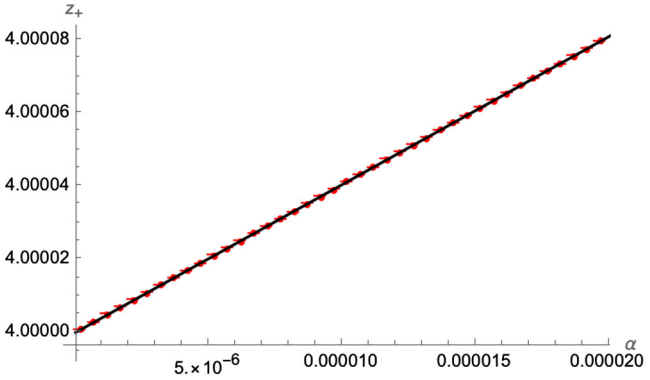

FIG. 11. Numerical position of the position of the horizon z_+ as a function of α for $\chi = 2$ and $\Omega_1 > 0$.

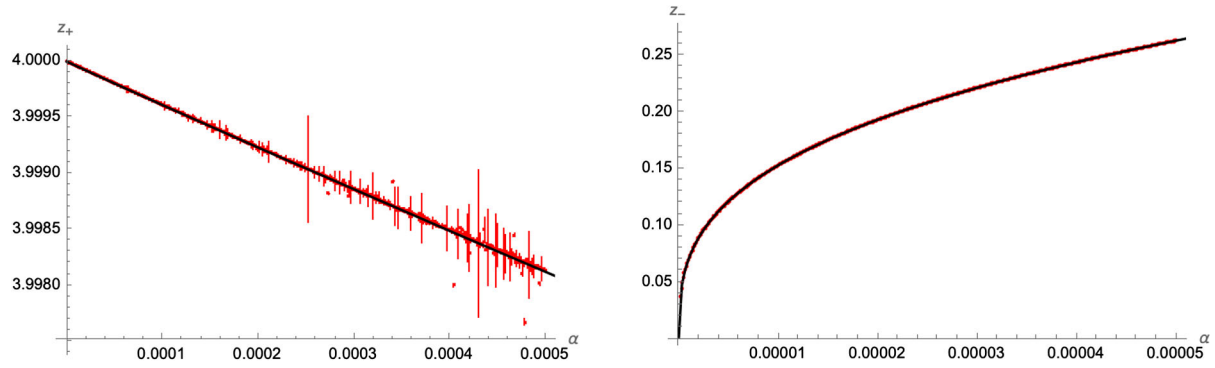

FIG. 12. Numerical position of the position of the horizon z_+ (left panel) and z_- (right panel) as a function of α for $\chi = 2$ and $\Omega_1 < 0$.

$$z_+ = 4(\bar{a}_1 + \bar{a}_2\alpha + \bar{a}_3\alpha^{3/2}). \quad \text{with} \quad \begin{aligned} 4\bar{a}_1 &= 4 \pm 2.2 * 10^{-9}, \\ 4\bar{a}_2 &= 4.0036 \pm 0.007, \\ 4\bar{a}_3 &= 7.853 \pm 2.523. \end{aligned} \tag{A3}$$

The numerical results for $\bar{a}_1$ and $\bar{a}_2$ are compatible with the coefficients obtained for the zeroes of f_1, while the coefficient $\bar{a}_3$ is not (namely $a_1 = 1$, $a_2 = 1$ and $a_3 = -\frac{2}{\pi} \sim -0.637$). This suggests, that the corrections to the position of the horizon z_+ that stem from using the improved metric function $\bar{f}_1$ are of order $\mathcal{O}(\alpha^{3/2})$.

(ii) $\Omega_1 < 0$: In this case, the two zeroes of $\bar{f}_1$ as a function of α (for $\chi = 2$) are plotted in Fig. 12 for $\chi = 2$. The solid black line is approximated by

$$z_+ = 4(\bar{a}_1 + \bar{a}_2\alpha + \bar{a}_3\alpha^{3/2}), \quad \text{with} \quad \begin{aligned} 4\bar{a}_1 &= 4 \pm 4.8 * 10^{-7}, \\ 4\bar{a}_2 &= -3.979 \pm 0.045, \\ 4\bar{a}_3 &= 9.947 \pm 2.685, \end{aligned} \tag{A4}$$

$$z_- = \bar{b}_1\alpha^{\frac{1}{3}} + \bar{b}_2\alpha^{\frac{2}{3}} + \bar{b}_3\alpha + \bar{b}_4\alpha^{\frac{4}{3}}, \quad \text{with} \quad \begin{aligned} \bar{b}_1 &= 7.0827 \pm 0.00005, \\ \bar{b}_2 &= 1.6724 \pm 0.0114. \\ \bar{b}_3 &= 2.26 \pm 0.60, \\ \bar{b}_4 &= 4.45 \pm 9.08. \end{aligned} \tag{A5}$$

For the position of the outer horizon z_+, the situation is similar to the case $\Omega_1 > 0$: the coefficients $\bar{a}_{1,2}$ are numerically compatible with the values $a_{1,2}$ coming from f_1, while $\bar{a}_3$ is not. This suggests, that the corrections to the position of the horizon z_+ that stem from using the improved metric function $\bar{f}_1$ are of order $\mathcal{O}(\alpha^{3/2})$. For z_- the coefficients $\bar{b}_{1,2,3}$ are numerically compatible with the values obtained from f_1. In view of the large numerical uncertainty, this suggests that the corrections to the position of the inner horizon appear at an order larger than $\mathcal{O}(\alpha)$.

3. Second order quantum corrections

Before treating the second order quantum corrections, we first provide a relation between the proper distances d_1 and d_0: we start from the definition of d_1 in (19), however, instead of a function of z we consider it as a function of d_0 defined in (11).[8] We then find for the first derivative

$$\frac{\mathrm{d}d_1}{\mathrm{d}z} = \frac{\mathrm{d}d_1}{\mathrm{d}d_0}\frac{\mathrm{d}d_0}{\mathrm{d}z} = \frac{1}{\sqrt{|1 - \frac{2\chi}{z}(1 + \frac{\Omega_1}{d_0^2})|}}. \tag{A6}$$

Using (10) we therefore find

$$\frac{\mathrm{d}d_1}{\mathrm{d}d_0} = \sqrt{\frac{|1 - \frac{2\chi}{z}|}{|1 - \frac{2\chi}{z}(1 + \frac{\Omega_1}{d_0^2})|}} \tag{A7}$$

where implicitly z is understood as a function of d_0. We can consider two limits of this equation

[8]This is possible since d_0 is a monotonic function in z.

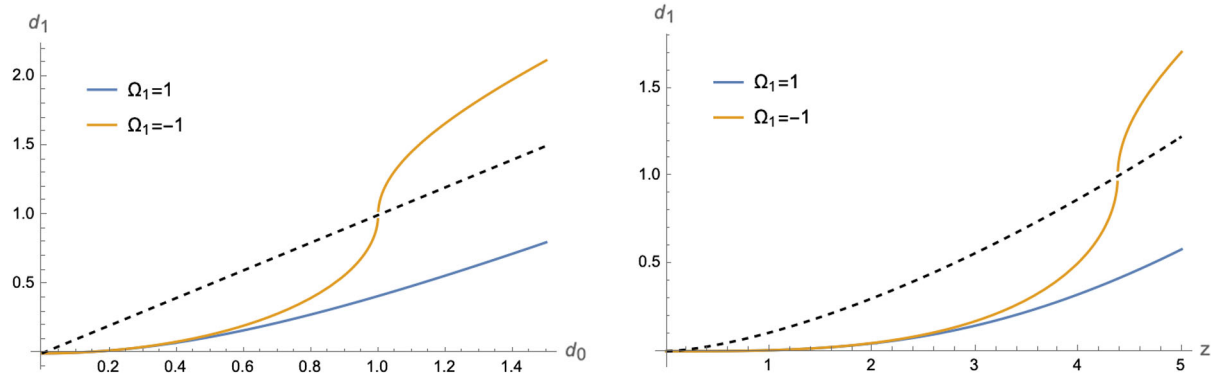

FIG. 13. Distance d_1 in Eq. (A10) as a function of d_0 (left panel) and of z assuming that $\chi = 20$ (right panel). The dashed black line corresponds to d_0 for comparison.

(i) $\chi \ll z$ (or equivalently $\chi \ll d_0$): in this case, the Eq. (A7) becomes

$$\frac{\mathrm{d}d_1}{\mathrm{d}d_0} = 1, \tag{A8}$$

which has as solution $d_1 \sim d_0$, i.e., for distances far away from the BH the two distances become equivalent.

(ii) $\chi \gg z$ (or equivalently $\chi \gg d_0$): in this case, the Eq. (A7) becomes

$$\frac{\mathrm{d}d_1}{\mathrm{d}d_0} = \sqrt{\frac{1}{|1+\frac{\Omega_1}{d_0^2}|}}, \tag{A9}$$

which is a differential equation for d_1 and can be integrated up in a direct fashion[9]

$$d_1 = \begin{cases} d_0\sqrt{1+\frac{\Omega_1}{d_0^2}} - \sqrt{\Omega_1} & \text{if} \quad \Omega_1 > 0, \\ \sqrt{-\Omega_1} - d_0\sqrt{-\frac{\Omega_1}{d_0^2}-1} & \text{if} \quad \Omega_1 < 0 \text{ and } d_0 < \sqrt{-\Omega_1}), \\ \sqrt{-\Omega_1} + d_0\sqrt{1+\frac{\Omega_1}{d_0^2}} & \text{if} \quad \Omega_1 < 0 \text{ and } d_0 > \sqrt{-\Omega_1}). \end{cases} \tag{A10}$$

Here the integration constants have been chosen in such a way that d_1 is a continuous function of d_0 and $\lim_{d_0\to 0} d_1 = 0$. Graphically, the solutions are shown in Fig. 13. For small values of d_0 we find

$$d_1 \sim \frac{d_0^2}{2\sqrt{|\Omega_1|}} + \mathcal{O}(d_0^4). \tag{A11}$$

We can now turn to the second order quantum corrections. To this end, we generalize the differential equation (A7) for d_2 (as a function of d_1)

$$\frac{\mathrm{d}d_2}{\mathrm{d}d_1} = \sqrt{\frac{|1-\frac{2\chi}{z}(1+\frac{\Omega_1}{d_0^2})|}{|1-\frac{2\chi}{z}(1+\frac{\Omega_1}{d_1^2}+\frac{\Omega_2}{d_1^4})|}}. \tag{A12}$$

As before, we can consider two limits of this equation

(i) $\chi \ll z$ (or equivalently $\chi \ll d_1$): in this case, the Eq. (A12) becomes

$$\frac{\mathrm{d}d_2}{\mathrm{d}d_1} = 1, \tag{A13}$$

which has as solution $d_2 \sim d_1$, i.e., for distances far away from the BH the two distances become equivalent.

(ii) $\chi \gg z$ (or equivalently $\chi \gg d_1$): in this case, the Eq. (A12) becomes

$$\frac{\mathrm{d}d_2}{\mathrm{d}d_1} = \sqrt{\frac{|1+\frac{\Omega_1}{d_0^2}|}{|1+\frac{\Omega_1}{d_1^2}+\frac{\Omega_2}{d_1^4}|}}. \tag{A14}$$

which together with (A10) is a differential equation for d_2 and can in principle be integrated as a function for d_1. Since this is, however, technically difficult, we focus on expanding d_2 around $d_1 = 0$ and for simplicity focus on the case $\Omega_{1,2} > 0$[10]:

[9]Requiring d_1 to be u independent implies also independence of Ω_1 on u.

[10]Other cases can be analyzed in a similar fashion.

$$\frac{\mathrm{d}d_2}{\mathrm{d}d_1} = \sqrt{\frac{1+\frac{\Omega_1}{d_1(d_1+2\sqrt{\Omega_1})}}{1+\frac{\Omega_1}{d_1^2}+\frac{\Omega_2}{d_1^4}}}. \tag{A15}$$

Expanding for small d_1 (or equivalently small d_0), we find

$$\begin{aligned} d_2 &\sim \frac{\sqrt{2}}{5}\frac{\Omega_1^{1/4}}{\sqrt{\Omega_2}} d_1^{5/2} + \mathcal{O}(d_1^{7/2}) \\ &\sim \frac{d_0^5}{20\Omega_1\sqrt{\Omega_2}} + \mathcal{O}(d_0^7), \end{aligned} \tag{A16}$$

which is indeed compatible with (28).

[1] C. P. Burgess, Quantum gravity in everyday life: General relativity as an effective field theory, Living Rev. Relativity **7**, 5 (2004).

[2] Lin-Yuan Chen, Nigel Goldenfeld, and Y. Oono, Renormalization group and singular perturbations: Multiple scales, boundary layers, and reductive perturbation theory, Phys. Rev. E **54**, 376 (1996).

[3] Lin-Yuan Chen, Nigel Goldenfeld, and Y. Oono, Renormalization group theory and variational calculations for propagating fronts, Phys. Rev. E **49**, 4502 1994).

[4] G. I. Barenblatt, Self-similarity: Similarity and intermediate asymptotic form, Radiophys. Quantum Electron. **19**, 643 (1976).

[5] Sidney R. Coleman and Erick J. Weinberg, Radiative corrections as the origin of spontaneous symmetry breaking, Phys. Rev. D **7**, 1888 (1973).

[6] A. B. Migdal, Vacuum polarization in strong non-homogeneous fields, Nucl. Phys. **B52**, 483 (1973).

[7] D. J. Gross and Frank Wilczek, Asymptotically free gauge theories—I, Phys. Rev. D **8**, 3633 (1973).

[8] Heinz Pagels and E. Tomboulis, Vacuum of the quantum Yang-Mills theory and magnetostatics, Nucl. Phys. **B143**, 485 (1978).

[9] Sergei G. Matinyan and G. K. Savvidy, Vacuum polarization induced by the intense gauge field, Nucl. Phys. **B134**, 539 (1978).

[10] Stephen L. Adler, Short distance perturbation theory for the leading logarithm models, Nucl. Phys. **B217**, 381 (1983).

[11] W. Dittrich and M. Reuter, *Effective Lagrangians in Quantum Electrodynamics*, Lecture Notes in Physics (Springer Berlin Heidelberg, 1985), Vol. 220.

[12] Kenneth G. Wilson, Renormalization group and critical phenomena. 1. Renormalization group and the Kadanoff scaling picture, Phys. Rev. B **4**, 3174 (1971).

[13] Kenneth G. Wilson, Renormalization group and critical phenomena. 2. Phase space cell analysis of critical behavior, Phys. Rev. B **4**, 3184 (1971).

[14] Alfio Bonanno and Martin Reuter, Renormalization group improved black hole space-times, Phys. Rev. D **62**, 043008 (2000).

[15] Alessia Platania, Dynamical renormalization of black-hole spacetimes, Eur. Phys. J. C **79**, 470 (2019).

[16] John F. Donoghue, A critique of the asymptotic safety program, Front. Phys. **8**, 56 (2020).

[17] John F. Donoghue, Leading Quantum Correction to the Newtonian Potential, Phys. Rev. Lett. **72**, 2996 (1994).

[18] John F. Donoghue, General relativity as an effective field theory: The leading quantum corrections, Phys. Rev. D **50**, 3874 (1994).

[19] John F. Donoghue, Introduction to the effective field theory description of gravity, in *Advanced School on Effective Theories* (1995), arXiv:gr-qc/9512024.

[20] John F. Donoghue and Basem Kamal El-Menoufi, QED trace anomaly, non-local Lagrangians and quantum equivalence principle violations, J. High Energy Phys. 05 (2015) 118.

[21] John F. Donoghue and Basem Kamal El-Menoufi, Nonlocal quantum effects in cosmology: Quantum memory, nonlocal FLRW equations, and singularity avoidance, Phys. Rev. D **89**, 104062 (2014).

[22] John F. Donoghue and Basem Kamal El-Menoufi, Covariant non-local action for massless QED and the curvature expansion, J. High Energy Phys. 10 (2015) 044.

[23] A. O. Barvinsky and G. A. Vilkovisky, The generalized Schwinger-Dewitt technique in gauge theories and quantum gravity, Phys. Rep. **119**, 1 (1985).

[24] A. O. Barvinsky and G. A. Vilkovisky, The generalized Schwinger-De Witt technique and the unique effective action in quantum gravity, Phys. Lett. B **131B**, 313 (1983).

[25] A. O. Barvinsky and G. A. Vilkovisky, Beyond the Schwinger-Dewitt technique: Converting loops into trees and in-in currents, Nucl. Phys. **B282**, 163 (1987).

[26] A. O. Barvinsky and G. A. Vilkovisky, Covariant perturbation theory. 2: Second order in the curvature. General algorithms, Nucl. Phys. **B333**, 471 (1990).

[27] A. O. Barvinsky, Yu. V. Gusev, G. A. Vilkovisky, and V. V. Zhytnikov, Asymptotic behaviors of the heat kernel in covariant perturbation theory, J. Math. Phys. (N.Y.) **35**, 3543 (1994).

[28] I. G. Avramidi, The covariant technique for calculation of one loop effective action, Nucl. Phys. **B355**, 712 (1991); **B509**, 557(E) (1998).

[29] Alessandro Codello, Jakob Joergensen, Francesco Sannino, and Ole Svendsen, Marginally deformed Starobinsky gravity, J. High Energy Phys. 02 (2015) 050.

[30] Basem Kamal El-Menoufi, Quantum gravity of Kerr-Schild spacetimes and the logarithmic correction to Schwarzschild black hole entropy, J. High Energy Phys. 05 (2016) 035.

[31] Salvatore Capozziello and Maurizio Capriolo, Gravitational waves in non-local gravity, Classical Quantum Gravity **38**, 175008 (2021).

[32] Salvatore Capozziello and Francesco Bajardi, Non-local gravity cosmology: An overview, Int. J. Mod. Phys. D **31**, 2230009 (2022).

[33] Aaron Held, Invariant renormalization-group improvement, arXiv:2105.11458.
[34] Sean M. Carroll, *Spacetime and Geometry* (Cambridge University Press, Cambridge, England, 2019).
[35] P. K. Townsend, Black holes: Lecture notes, arXiv:gr-qc/9707012.
[36] S. W. Hawking, Particle creation by black holes, Commun. Math. Phys. (N.Y.) **43**, 199 (1975); **46**, 206(E) (1976).
[37] Dmitri V. Fursaev, Temperature and entropy of a quantum black hole and conformal anomaly, Phys. Rev. D **51**, R5352 (1995).
[38] Romesh K. Kaul and Parthasarathi Majumdar, Logarithmic Correction to the Bekenstein-Hawking Entropy, Phys. Rev. Lett. **84**, 5255 (2000).
[39] Steven Carlip, Logarithmic corrections to black hole entropy from the Cardy formula, Classical Quantum Gravity **17**, 4175 (2000).
[40] Niels Emil Jannik Bjerrum-Bohr, John F. Donoghue, and Barry R. Holstein, Quantum corrections to the Schwarzschild and Kerr metrics, Phys. Rev. D **68**, 084005 (2003); **71**, 069904(E) (2005).
[41] S. D. Odintsov and I. L. Shapiro, General relativity as the low-energy limit in higher derivative quantum gravity, Classical Quantum Gravity **9**, 873 (1992).
[42] E. Elizalde, S. D. Odintsov, and I. L. Shapiro, Asymptotic regimes in quantum gravity at large distances and running Newtonian and cosmological constants, Classical Quantum Gravity **11**, 1607 (1994).
[43] Arif Akhundov and Anwar Shiekh, A review of leading quantum gravitational corrections to Newtonian gravity, Electron. J. Theor. Phys. **5**, 1 (2008).
[44] Benjamin Knorr and Alessia Platania, Sifting quantum black holes through the principle of least action, Phys. Rev. D **106**, L021901 (2022).